Historical trends in pH and carbonate biogeochemistry on the Belize Mesoamerican Barrier Reef System

S. Fowell[1], G. L. Foster[1], J. Ries[2], K. D. Castillo[3], E. de la Vega[1], T. Tyrrell[1], H. K. Donald[1], T.B. Chalk[1].

[1] Ocean and Earth Science, National Oceanography Centre Southampton, University of Southampton, European Way, Southampton SO14 3ZH, UK.

[2] Marine Science Center, Northeaster University, 430 Nahant Rd, Nahant, MA 01908, USA.

[3] Marine Sciences, University of North Carolina at Chapel Hill, Chapel Hill NC 27599-3300, USA.

Corresponding author: G.L. Foster (Gavin.Foster@noc.soton.ac.uk)

Key Points:

- B and C isotope analyses of the reef-building coral *S. siderea* reveal reef-scale patterns of pH, NEC and NEP.
- Declining coral extension is not associated with ocean acidification.
- NEC was enhanced in the backreef in the 1920-1940s, NEP was enhanced in the forereef since 1980s.

This article has been accepted for publication and undergone full peer review but has not been through the copyediting, typesetting, pagination and proofreading process which may lead to differences between this version and the Version of Record. Please cite this article as doi: 10.1002/2017GL076496

Abstract

Coral reefs are important ecosystems that are increasingly negatively impacted by human activities. Understanding which anthropogenic stressors play the most significant role in their decline is vital for the accurate prediction of future trends in coral reef health and for effective mitigation of these threats. Here we present annually resolved boron and carbon isotope measurements of two cores capturing the past 90 years of growth of the tropical reef-building coral *Siderastrea siderea* from the Belize Mesoamerican Barrier Reef System. The pairing of these two isotope systems allows us to parse the reconstructed pH change into relative changes in net ecosystem productivity and net ecosystem calcification between the two locations. This approach reveals that the relationship between seawater pH and coral calcification, at both a colony and ecosystem level, is complex and cannot simply be modeled as linear or even positive. This study also underscores both the utility of coupled $\delta^{11}B$-$\delta^{13}C$ measurements in tracing past biogeochemical cycling in coral reefs and the complexity of this cycling relative to the open ocean.

1 Introduction

1.1. Ocean acidification and coral reefs

Ocean acidification (OA) in response to anthropogenic emissions of CO_2 has been shown to negatively impact marine calcifiers (e.g., *Gattuso et al.* [2015]). Coral reefs account for around 50% of shallow water $CaCO_3$ production (ca. 0.7 Pg of $CaCO_3$ per year), protect shorelines from storms and rising sea-level, generate trillions of dollars in tourism worldwide, and the ecosystems that they support feed millions of people [*Costanza et al.*, 2014]. However, the effect of OA on $CaCO_3$ production and dissolution on coral reefs remains unclear. This is despite a conceptually simple positive relationship between ocean pH ($-\log_{10}$ [H+]) and the saturation state (Ω) of aragonitic $CaCO_3$, defined as:

$$\Omega_{aragonite} = \frac{[Ca^{2+}] * [CO_3^{2-}]}{K^*_{aragonite}} \qquad [1a]$$

$$CO_{2(aq)} + H_2O \leftrightarrow HCO_3^- + H^+ \leftrightarrow CO_3^{2-} + 2H^+ \qquad [1b]$$

where $[Ca^{2+}]$ and $[CO_3^{2-}]$ are the calcium and carbonate ion concentration in seawater, respectively, and $K^*_{aragonite}$ is the solubility product of aragonite in seawater. Part of the uncertainty in the future response of coral reef calcification to OA is due to the high degree of natural variability in the ocean carbonate system that occurs in coral reefs [*DeCarlo et al.*, 2017]. In particular, it is recognised that the balance between net ecosystem production (NEP = gross primary production – autotrophic and heterotrophic respiration) and net ecosystem calcification (NEC = gross calcification – gross $CaCO_3$ dissolution) modulates the carbon chemistry of these complex ecosystems. CO_2 is both the product of calcification and the principal reactant in photosynthesis, therefore these two processes can in principal be linked and feedbacks may exist such that anthropogenic or natural changes in CO_2 could alleviate or amplify the influence of OA on the inhabitants of a reef (e.g., *Yeakal et al.*, [2015]).

The balance between NEP and NEC, and its evolution through time, can be investigated through measurements of total alkalinity (ALK) and total dissolved inorganic carbon (DIC) in reef waters (e.g., *Bates et al.* [2010]). Unfortunately, such monitoring of the "health" of coral reefs has only recently begun and instrumental records longer than ca. 5 years are rare. Those longer term records that do exist tend to be characterised by considerable gaps in sampling (e.g., *Silverman et al.* [2012]*; Silverman et al.* [2014]), with the longest continual record thus far restricted to the last 20 years [*Bates*, 2017]. As a

consequence, the full impact of the acidification that has occurred over the last 100 years (ca. 0.1 pH units in the open ocean; *Bates et al.* [2014]), and the ability (or lack thereof) of reef systems to modulate their carbonate biogeochemistry against this apparent threat, remains largely unknown.

1.2. Proxy constraints on NEP and NEC variability

Reliable observations of the carbonate chemistry of coral reefs prior to the 1980s do not exist. It is therefore unlikely that the ecosystem level response of coral reefs to historic anthropogenic oceanic change can be estimated from direct measurements. Instead, we must turn to geochemical proxies. One such proxy that has received much attention is the boron isotope pH proxy (e.g., *Goodkin et al.* [2015]*; Liu et al.* [2014]; *Wei et al.* [2009]; *Pelejero et al.* [2005]). There are two aqueous species of boron in seawater (boric acid and borate ion), and their relative abundance depends primarily on pH [*Dickson*, 1990]. Boron has two stable isotopes, ^{11}B and ^{10}B, and a strong isotopic fractionation exists between boric acid and borate ion (ca. 27.2 ‰; *Klochko et al.* [2006]). This causes the isotopic composition of the two aqueous species of boron to also vary with pH as their relative abundance changes (see *Foster and Rae* [2016] for more details). The following relationship can thus be defined:

$$pH = pK_B^* - \log\left(-\frac{\delta^{11}B_{(sw)} - \delta^{11}B_{bor}}{\delta^{11}B_{(sw)} - \alpha_B\delta^{11}B_{bor} - \varepsilon_B}\right) \qquad [2]$$

where pK^*_B is the $-\log_{10}$ of the stoichiometric equilibrium constant for boron dissociation in seawater ($pK^*_B \approx 8.6$ in seawater at 25 ^oC, 35 psu salinity and atmospheric pressure [*Dickson*, 1990]), $\delta^{11}B_{sw}$ is the boron isotopic composition of seawater (39.61 ‰; *Foster et al.* [2010]), $\delta^{11}B_{bor}$ is the boron isotopic composition of seawater borate ion, and α_B and ε_B are expressions of the magnitude of isotopic fractionation between the two aqueous species of boron (1.0272 and 27.2, respectively; *Klochko et al.* [2006]).

Recent experiments have shown that only the borate ion is incorporated into inorganic aragonite [*Noireaux et al.*, 2015], and that this process occurs with little or no isotope fractionation, allowing substitution of aragonite $\delta^{11}B$ for $\delta^{11}B_{bor}$ in equation [2] and the calculation of the pH at which the aragonite precipitated. A complicating factor of using boron isotopes in coral aragonite, however, is the influence of coral physiology and the elevation of pH within the calcifying fluid (pH_{cf}) by the coral [*Venn et al.*, 2013], such that $\delta^{11}B$ of the coral skeleton ($\delta^{11}B_{coral}$) represents $\delta^{11}B_{bor}$ of the calcifying fluid rather than $\delta^{11}B_{bor}$ of seawater [*McCulloch et al.*, 2012*; Holcomb et al.*, 2014]. Nevertheless, because changes in seawater pH have been shown to cause changes in coral calcifying fluid pH (e.g., *Ries* [2011]), coral skeletal $\delta^{11}B$ tracks seawater $\delta^{11}B_{bor}$ and there is a consistent relationship between internal and external pH (e.g., *Halcomb et al.* [2014]). This permits the reconstruction of seawater pH at annual resolution from the boron isotope composition of coral skeletons using species specific $\delta^{11}B$-pH calibrations (e.g., *Liu et al.* [2014]; *Trotter et al.* [2011]).

Although surface ocean pH has declined by ca. 0.1 pH units over the last 100 years, pH on a coral reef is also intimately related to local physical and biogeochemical processes that change the relative concentrations of ALK and DIC, the residence time of seawater on the reef, and water depth (e.g., *Bates et al.* [2010]; Figure 1). Indeed, water column pH on a coral reef can vary up to ± 0.5 pH units on daily, monthly and seasonal timescales (e.g., *DeCarlo et al.* [2017]; *Drupp et al.* [2013]). Although CO_2 outgassing (and, conversely, CO_2

invasion), and benthic processes can impact seawater pH on a reef, the main factors controlling this pH variability are temporal variations in NEC and NEP, which themselves reflect the addition/removal of DIC and ALK by reef biology, but also water residence time and water depth [*Bates et al.*, 2010*; DeCarlo et al.*, 2017*; Gattuso et al.*, 1999]. This strong biological control of coral reef pH (Figure 1) complicates the reconstruction of long-term open-ocean pH trends from the boron isotopic composition of long-lived tropical corals, and likely accounts for the annual and decadal variability in existing $\delta^{11}B$-derived seawater pH records (Supplementary Figure 1). Although the complex carbonate chemistry of coral reef systems complicates paleo-pH reconstruction from coral $\delta^{11}B$, it affords an opportunity to reconstruct past changes in NEC and NEP within these critical ecosystems.

As shown in Figure 1, seawater pH can be affected by modifying NEC and/or NEP and, as noted by *Yeakel et al.* [2015], pH on its own cannot distinguish the process(es) responsible for any observed change in seawater carbonate chemistry. We assert that the carbon isotopic composition ($\delta^{13}C$) of the coral skeleton can provide critical information in this regard, allowing a more nuanced view of the temporal evolution of the seawater carbonate system, because, unlike pH, the $\delta^{13}C$ of seawater DIC is only significantly altered by variations in NEP and is unaffected by NEC (Figure 1). Although it is unclear to what extent coral skeleton $\delta^{13}C$ reflects $\delta^{13}C$ of seawater DIC, which may also be influenced by a number of "vital effects" [*Swart*, 1983*; McConnaughy*, 1989*; Allison et al.*, 1996*; Gagan et al.*, 1994*; Reynaud et al.*, 2004; *Meibom et al*. 2006; *Krief et al.*, 2010*; Martin et al.*, 2016], *Swart et al.* [2010] showed that 78% of 37 colonies of several species of tropical corals exhibited a decline in $\delta^{13}C$ over the past century, consistent with their $\delta^{13}C$ being driven predominantly by the invasion of isotopically light anthropogenic carbon into the atmosphere and oceans – the so-called Suess effect [*Keeling et al.*, 1979]. That most tropical corals exhibit a steady decline in $\delta^{13}C$ over the past century implies an overriding sensitivity of coral $\delta^{13}C$ to the changing $\delta^{13}C$ of seawater DIC – regardless of whether that variability is driven by the Suess effect or changing NEP (Figure 1).

Here we use paired measurements of $\delta^{13}C$ and $\delta^{11}B$ of the skeleton of the scleractinian coral *Siderastrea siderea* sampled at an annual resolution to provide an understanding of how reef pH and patterns of NEP and NEC varied across the Sapodilla Cayes region of the Mesoamerican Barrier Reef System (MBRS) in Belize over the last 90 years. These results provide key insights into the impact of OA on *S. siderea* and demonstrate the utility of these two proxies in tracing the "health" of coral reef systems beyond the reach of the instrumental record.

2 Materials and Methods

Two cores were obtained in December 2009 from forereef (FR-02; 16.13715°N, 88.252883°W) and backreef (BR-06; 16.14045°N, 88.26015°W) colonies of *S. siderea* growing at 3 to 5 m water depth within Sapodilla Cayes region of the MBRS (*Castillo et al.* [2011]; Supplementary Figure 2). Consistent with global trends, coral cover on the MBRS is in decline [*Gardner et al.*, 2003], although the exact cause(s) is (are) currently widely debated [*Hughes*, 1994*; McClanahan et al.*, 1999*; Aronson et al.*, 2002]. Methods for sub-sampling of coral cores to separate annual growth bands, x-raying, and age-dating are described in *Castillo et al.* [2011]. Further sampling protocols and analytical methodology for $\delta^{11}B$ and $\delta^{13}C$ are described further in the Supplementary Information Text S1.

The $\delta^{11}B$ compositions of the forereef and backreef corals were used to calculate pH_{cf} using a modified version of equation [2]:

$$pH_{cf} = pK_B^* - \log\left(-\frac{\delta^{11}B_{(sw)} - \delta^{11}B_{coral}}{\delta^{11}B_{(sw)} - \alpha_B\delta^{11}B_{coral} - \varepsilon_B}\right) \qquad [3]$$

pK^*_B was determined for each sample based on the sea surface temperature from the HadISST1 dataset (*Rayner et al.*, [2003]). Salinity has a very minor effect on calculated pH and so was assumed to be constant at 35 psu. All carbonate system calculations were made using the R package "seacarb" [*Lavigne and Gattuso*, 2010]

There is currently no $\delta^{11}B$-pH calibration for *S. siderea*. Instead, we use equations developed for the coral species *Porites cylindrica* [*Trotter et al.*, 2011; *McCulloch et al.*, 2012; *Liu et al.*, 2014] to estimate seawater pH (pH_{sw}) from the pH_{cf}:

$$pH_{sw} = \frac{(pH_{cf} - 4.72)}{0.466} \qquad [4]$$

This choice of calibration determines the absolute pH but has little influence on relative pH change, which is the focus of the present work (see below and Supplementary Figure 3; *Foster and Rae* [2016]). In order to isolate the long-term trends in the 1912-2008 time-series, reconstructed pH_{sw} values were fitted with LOESS smoothers in R, with the degree of smoothing determined via generalized cross-validation.

3 Results and Discussion

3.1. $\delta^{11}B$-derived seawater pH and $\delta^{13}C$ timeseries from the MBRS

Both the forereef (FR-02) and backreef (BR-06) core exhibit a decline in $\delta^{13}C$ of 1 to 1.5 ‰ over the last ca. 100 years, albeit with an offset between them of around 0.4 ‰ that increased since the 1980s (Figure 2). This broad temporal evolution is in good agreement with other coral studies (e.g. *Böhm et al.* [2002]; *Swart et al.* [2010]) and is similar to trends observed in the atmosphere [*Rubino et al.*, 2013] over a comparable interval. Both Belize coral $\delta^{13}C$ records, however, display considerable inter-annual variability (Figure 2) with an apparent ca. 8 year cyclicity (Supplementary Figure 4). This is consistent with the assertion that the long-term trend of the $\delta^{13}C$ timeseries recorded in these two corals reflects the uptake of

isotopically light anthropogenic CO_2, with short-term variability reflecting either local variability in DIC $\delta^{13}C$ or non-DIC influences on coral $\delta^{13}C$ (Figure 2).
The $\delta^{11}B$ timeseries for the two coral cores are surprisingly distinct (Figure 2), despite their geographic proximity (Supplementary Figure 2). Specifically, the forereef coral (FR-02) exhibits no consistent long-term trend (p=0.41), but exhibits the same quasi-decadal variability evident in the $\delta^{13}C$ records (Supplementary Figure 4). In contrast, the backreef coral (BR-06) exhibits a consistent decline in $\delta^{11}B$ over the same interval (ca. -1.2‰ per 100 years; Figure 2), while exhibiting less short-term variability than observed for FR-02 (Supplementary Figure 4). Given the overriding influence of external pH on the $\delta^{11}B$ of coral aragonite (equations 2-4), these disparate $\delta^{11}B$ records imply vastly different trends in seawater pH at the two core locations.

The $\delta^{11}B$ record within each core was converted to a pH timeseries using equations [3] and [4] (Figure 2). Although the lack of a species-specific $\delta^{11}B$-pH calibration for *S. siderea* means absolute values of the reconstructed seawater pH should be interpreted with caution, the observed trends in seawater pH can be interpreted with confidence (Supplementary Figure 3). This analysis suggests that seawater pH at site of the backreef coral decreased over the last ca. 100 years from 8.05 to 7.87, with an average decline of -0.016 pH units per decade (determined by linear regression). This rate of acidification accelerated to -0.019 ± 0.006 units per decade (p = 0.009) after 1970 – similar to that of the open North Atlantic as measured by the Bermuda Atlantic Timeseries for the interval 1983-2014 (-0.017 ± 0.001 per decade; *Bates et al.*, [2014]) and the nearby Cariaco Basin for the interval 1995-2014 (-0.025 ± 0.004 per decade; Table S1). Although the more recent portion of the backreef pH record matches seawater pH trends expected from records of atmospheric pCO_2, the interval of marked acidification from 1920 to 1940 in the backreef core is much higher than expected given the atmospheric pCO_2 record (Figure 2). In contrast, the forereef core exhibits no significant long-term pH trend over the same interval (-0.004 ± 0.004 per decade, p = 0.36) or since 1970 (-0.002 ± 0.02 per decade; p = 0.946).

3.2 Relationship between linear extension and seawater pH for *S. siderea*

Castillo et al. [2011] found that over the last 100 years, there was a marked regional-scale decline in linear extension for forereef *S. siderea* of the southern MBRS, averaging around -0.2 cm/year, while extension in backreef corals increased by 0.1 cm/yr. Given the close relationship between rates of linear extension and rates of calcification that exist in this species [*Carricart-Ganivet et al.*, 2013], this provides the opportunity to assess how calcification of *S. siderea* has responded to the OA that it has experienced over the last 100 years (Supplementary Figure 5). Contrary to expectation (e.g., *McCulloch et al.* [2012]), we find no statistically significant relationship (p=0.5) between extension rates and reconstructed seawater pH (Supplementary Figure 5) for the forereef coral and a strong *inverse* correlation (p=<0.001) for the backreef coral (i.e., increasing extension with decreasing pH; Supplementary Figure 5).

The contrasting relationship between seawater pH and extension rate for the backreef and forereef corals (Figure 2d, Supplementary Figure 5) suggests that OA has not had an obviously detrimental effect on the calcification of *S. siderea* over the last 100 years in the Sapodilla Cayes. This finding agrees with the recent culturing experiment of *Castillo et al.* [2014] that showed that for moderate rates of acidification, calcification in this species is enhanced, possibly due to increased availability of dissolved CO_2 for symbiont photosynthesis. Although this suggests that *S. siderea* on the MBRS is apparently resilient to

moderate OA, the laboratory experiments also revealed that there is a limit to the degree to which increased CO_2 availability for photosynthesis (i.e., decreased pH) offsets the deleterious effects of CO_2-induced reductions in $\Omega_{aragonite}$ on calcification in *S. siderea*. Nonetheless, other factors need to be investigated to determine what is responsible for the decline in forereef (but not backreef) *S. siderea* extension reported by *Castillo et al.* [2011].

3.3 Spatial patterns of pH and $\delta^{13}C$ on the MBRS

In order to compare the evolution of $\delta^{13}C$ and pH displayed by the two coral cores, we interpolate both cores to a common age scale and plot forereef-to-backreef pH difference (ΔpH) vs. forereef-to-backreef $\delta^{13}C$ difference ($\Delta^{13}C$; Figure 3). A linear regression fitted to $\Delta^{13}C$ and ΔpH is described by the following equation:

$$\Delta pH = \left(0.16 \pm 0.03 \cdot \Delta^{13}C\right) + 0.08 \pm 0.17 \quad (R^2 = 0.38, p = 0.00007) \quad [6]$$

This strong correlation between $\delta^{11}B$-derived pH and $\delta^{13}C$, as well as the apparent ca. 8-year cyclicity in both proxies (Supplementary Figure 4), is consistent with trends previously reported for single coral colonies (e.g., *Hemming et al.* [1998]). Examining the difference between the two cores in this way removes the inherent covariation in coral $\delta^{13}C$ and $\delta^{11}B$ driven by increasing anthropogenic CO_2: anthropogenic-CO_2-induced reductions in seawater DIC $\delta^{13}C$ [*Swart et al.*, 2010] via the Suess effect and reductions in seawater borate $\delta^{11}B$ via ocean acidification [*Sabine et al.*, 2004]. The residual correlation between pH and $\delta^{13}C$ between the cores (i.e., the correlation between $\Delta^{13}C$ and ΔpH) should therefore represent relative variations in NEP and NEC at the two core locations (e.g., Figure 1), thereby allowing reconstruction of trends in NEP and NEC at those locations through time. For simplicity, we ignore the possible influence of seawater pH on coral $\delta^{13}C$ that has been observed in some studies (e.g., *Martin et al.* [2016]; *Krief et al.* [2010]; *Spero et al.* [1997]) and assume that changes in coral $\delta^{13}C$ solely reflect changes in $\delta^{13}C$ of seawater DIC – which is reasonable given the relatively small change in pH experienced by the MBRS over the last 100 years (<0.2 pH units) and the relatively small impact that seawater pH and other non-DIC factors have on coral $\delta^{13}C$ (e.g. *Martin et al.* [2016]).

The observed positive relationship between $\Delta^{13}C$ and ΔpH is likely indicative of enhanced NEP and reduced NEC at the forereef core location relative to the backreef core location. More precise insights into the causes of such changes can, however, be identified provided the $\delta^{13}C$ of primary production and respiration are known (vertical contours on Figure 3). Values for biological tissue in coral reef ecosystems range from -17 to -31 ‰ [*Muscatine et al.*, 1989; *Reynaud et al.*, 2004; *Titlyanov et al.*, 2010; *Briand et al.*, 2014; *Carvalho et al.*, 2015] and here we use a value of -24 ‰, the median value from *Briand et al.* [2014], allowing us to contour Figure 3 for the removal/addition of DIC alone (i.e., change in NEP; black lines), as well as for the removal/addition of ALK:DIC with a 2:1 ratio (i.e., change in NEC; grey lines).

Projecting ΔpH and $\Delta^{13}C$ data onto the zero-contour of constant alkalinity effectively parses the pH change into that caused by NEC (only changes pH; Figure 3b) and that caused by NEP (changes pH and $\delta^{13}C$ of DIC; Figure 3c). This treatment reveals two important trends: (i) NEC was enhanced in the backreef, relative to the forereef, during the 1920s-1940s and (ii) NEP was enhanced in the forereef, relative to the backreef, since the 1980s. These

findings are largely irrespective of the specific δ^{11}B-pH calibration used and the δ^{13}C composition assigned to organic matter in the system.
This deconvolution of the pH signals into NEC and NEP variability also indicates that much of the quasi-decadal variability in pH at the forereef core is driven by differences in NEC between core locations – specifically, by ca. 8 year cycles in NEC in the forereef that cause corresponding cycles in forereef seawater pH (Supplementary Figure 4; Table S2). Cross correlation analysis of the detrended timeseries using the Pearson product moment correlation reveals a significant positive correlation (cor=0.44, p<0.001; Tables S2) between ΔpH from NEP and ΔpH from NEC, such that when NEC decreases in the forereef, NEP in that region also tends to increase. A similar pattern is revealed in long-term trends, albeit with a temporal offset: NEC was enhanced in the backreef compared to the forereef during the 1920s-1940s and NEP was enhanced in the forereef relative to the backreef since the 1980s.

It is important to recognize that these parameters can be influenced by both biological and physical mechanisms. For instance, the apparent increase in NEC in the backreef relative to the forereef could be caused by either an enhancement of calcification in the backreef (relative to the forereef) or an increase in the residence time of the water on the reef so the impact of calcification is proportionally enhanced (e.g., *DeCarlo et al.* [2017]). It is therefore important to consider both biological and physical oceanographic processes when inferring changes in NEC and NEP from δ^{11}B and δ^{13}C data.

Castillo et al. [2011] observed that rates of linear extension in *S. siderea* decreased in the forereef and increased in the backreef of the southern MBRS since the early 1900s. These trends in linear extension are therefore consistent with the observed reduction in forereef NEC and enhancement in backreef NEC through time being primarily driven by biological processes. It is also likely that the enhanced NEP in the forereef since the 1980s contributes to negating the open ocean OA signal evident in the backreef (BR-06) pH record. Similarly, the larger-than-expected pH change recorded in the backreef (BR-06) pH record, given historical changes in atmospheric pCO_2 (Figure 2), appears to be largely a consequence of enhanced NEC in the backreef – as observed at other backreef localities on shorter timescales (e.g., *Bates* [2017]).

A quasi-decadal (ca. 8-year) climate cycle in the Caribbean has been noted previously [*Jury*, 2009] in records of SST and rainfall. This mode of variability is considered distinct from the Pacific El Niño – Southern Oscillation (ENSO) and instead is related to slow oscillations of the North Atlantic Oscillation (NAO) driven by interactions between tropical Atlantic SST, the subtropical anticyclones, and the Hadley circulation [*Jury*, 2009]. For this mode of variability, warm SST in the Caribbean is typically equated with high rainfall. The HadISST record used here also shows a quasi-decadal ca. 8 year cycle when detrended (Supplementary Figures 4 & 6; Table S2) and is significantly positively correlated with detrended NEC (cor=0.37, p<0.001). These trends are consistent with *Castillo et al.*'s [2011] observation that linear extension of backreef *S. siderea* has been enhanced by warming over the past century, while linear extension of forereef *S. siderea* has been impaired by this warming – a dichotomy that they attribute to the increased thermal tolerance of the backreef populations that have historically experienced larger diurnal and seasonal temperature fluctuations relative to forereef populations that have historically experienced more stable temperatures.

Despite the strong correlation between NEP and NEC, the correlation between detrended NEP and detrended HadISST is not significant (cor=0.07, p=0.56; Table S2) – probably a result of the relatively small variability in NEP at this 8 year cycle and the low sampling

resolution (Supplementary Figure 6). However, area-averaged annual precipitation rates over the western Caribbean are significantly correlated with NEP (cor=0.30, p=0.003) but, unlike SST, are not significantly correlated with NEC (cor=0.15, p=0.16; Supplementary Figure 2 and Supplementary Figure 6; Table S2). However, limiting the area-averaged annual precipitation to land-only precipitation reveals the opposite pattern: a significant correlation with NEC (cor=0.38, p<0.001) but not with NEP (cor=0.14, p=0.19; Table S2).

These correlations suggest that SST and rainfall either influence NEC and NEP on the MBRS directly at the ecosystem level, or else indirectly by changing water residence time and/or water depth on the MBRS. Although we cannot identify the relative contributions of SST and rainfall to NEC and NEP with the data at hand, long-term anthropogenic processes may be forcing the reconstructed trends. For instance, the Caribbean experienced significant warming from 1910 to 1940, coincident with the first long-term increase in NEC preserved in the cores (Figure 3b, Supplementary Figure 7). *Jury* [2009] also noted a general increase in mean annual rainfall in the Caribbean since the 1960s and *Stephenson et al.* [2014] recorded a positive trend for the wider Caribbean in the interval of 1986-2010 for total annual precipitation, for average daily precipitation, and for heavy rainfall events. This secular increase in precipitation is coincident with the enhanced NEP evident in the forereef since the 1980s (Figure 3c). However it is important to note that *Stephenson et al.* [2014] did not find a significant precipitation trend for Belize itself, perhaps indicative of a more indirect, regional influence of precipitation on NEP, if not through residence time and water depth, possibly through sediment and nutrient supply via nearby rivers stimulating productivity.

The abundance of tropical corals has declined throughout the Caribbean and other reef systems around the world, with one regional study demonstrating that Caribbean coral cover declined from ca. 60% in the 1970s to ca. 10% by around 2000 [*Gardner et al.* 2003]. Although there are potentially numerous causes of this dramatic decline in coral health and abundance, these declines tend to be associated with expansion of macroalgae [*Schutte et al.*, 2010] and/or cyanobacterial mats into reef environments. It is therefore possible that the oscillations and long-term trends of enhanced precipitation and SST warming we observe here facilitated the expansion of non-calcifiers at the expense of calcifiers, thereby decreasing NEC and increasing NEP in some parts of the MBRS.

4 Conclusions

Boron isotopes measured within coral cores from the MBRS reveal that increasing atmospheric pCO_2 over the past 100 years has affected different parts of this reef system in very different ways: backreef environments have acidified in a manner consistent with, but in excess of, the open ocean while forereef environments have maintained relatively stable pH. Comparison with trends in linear extension also reveals that the relationship between seawater pH and coral calcification is complex, with declining pH associated with increasing extension in the backreef and constant pH in the forereef associated with declining extension in the forereef. Although counterintuitive, this finding is generally consistent with recent culture experiments showing that calcification in *S. siderea* is enhanced by moderate CO_2-induced reductions in seawater pH, possibly owing to CO_2-fertilisation of symbiotic zooxanthellae [*Castillo et al.,* 2014]. Although the cause of declining calcification in the forereef of the Belize region of the MBRS remains uncertain, our results suggest that ocean acidification can be ruled out.

Examination of spatial patterns in coral $\delta^{11}B$-derived seawater pH and $\delta^{13}C$ suggests that these systems can be used to reconstruct spatial variations in NEP and NEC through time. Although the complexity of vital effects for both isotope systems requires additional ground-truthing to improve the quantitative rigor of the approach, the general trends derived from the present study suggest that NEP increased in the forereef of the MBRS since the 1980s and that NEC increased in the backreef during the 1920s-1940s. The increased NEP in the forereef since the 1980s effectively countered the ocean acidification expected from anthropogenic increases in atmospheric pCO_2 over this interval. Conversely, the increased NEC in the backreef during the 1920s-1940s enhanced the anthropogenic acidification signal. Timeseries analysis revealed a quasi-decadal cycle in NEC and NEP that was correlated with oscillations in temperature and rainfall in the region. Our findings not only underscore the relatively untapped potential of using coupled analyses of $\delta^{11}B$-derived pH and $\delta^{13}C$ to trace key biogeochemical processes in coral reefs, they also highlight that, in contrast to the open ocean, the evolution of the carbonate system on coral reefs over the last century has not been controlled solely by anthropogenic CO_2.

Acknowledgments

S.E.F. and J.B.R. acknowledge laboratory assistance provided by Andy Milton at the University of Southampton and Travis Courtney of Northeastern University. This research was funded by the Natural Environment Research Council UK (Studentship number NE/K500926/1 to S.E.F.) and the National Oceanography Centre Southampton Graduate School. The collection, preparation, and carbon/oxygen isotopic analysis of the coral cores was funded by NOAA awards NA11OAR4310161/NA13OAR4310186 (to J.B.R. and K.D.C.) and NSF award 1437371 (to J.B.R.). This work was also partly funded by the Leverhulme Trust (award to G.L.F). Permits for collection and export of corals were granted by the Belize Fisheries Department, Government of Belize. Mark Jury (University of Puerto Rico) is thanked for supplying the precipitation data used in this study. This manuscript greatly benefited from reviews by Thomas DeCarlo and an anonymous reviewer. The data generated in this study are provided in Supplementary Table 3.

References

Allison, N., A. W. Tudhope, and A. E. Fallick (1996), Factors influencing the stable carbon and oxygen isotopic composition of *Porities lutea* coral skeletons from Phuket, South Thailand, *Coral Reefs*, *15*, 43-57.

Aronson, R., W. Precht, M. Toscano, and K. Koltes (2002), The 1998 bleaching event and its aftermath on a coral reef in Belize, *Mar. Biol., 141*, 435-447.

Bates, N. R. (2017), Twenty years of marine carbon cycle observations at devils hole Bermuda provide insights into seasonal hypoxia, coral reef calcification, and ocean acidification, *Front. Mar. Sci., 4*, 1-23.

Bates, N. R., A. Amat, and A. J. Andersson (2010), Feedbacks and responses of coral calcification on the Bermuda reef system to seasonal changes in biological processes and ocean acidification, *Biogeosciences, 7*, 2509-2530.

Bates, N. R., Y. M. Astor, M. J. Church, K. Currie, J. E. Dore, M. Gonzalez-Davila, L. Lorenzoni, F. Muller-Karger, J. Olafsson, and J. M. Santana-Casiano (2014), A time series view of changing ocean chemistry due to coean uptake of anthropogenic CO_2 and ocean acidification, *Oceanography*, *27*(1), 126-141.

Böhm, F., A. Haase-Schramm, A. Eisenhauer, W.-C. Dullo, M. M. Joachimski, and H. Lehnert (2002), Evidence for preindustrial variations in the marine surface water carbonate system from coralline sponges, *Geochemistry, Geophysics, Geosystems (G3)*, *3*(3), 10.1029/2001GC000264.

Briand, M. J., X. Bonnet, C. Goiran, G. Guillou, and Y. Letourneur (2015), Major sources of organic matter in a complex coral reef lagoon: identification from isotopic signatures ($\delta^{13}C$ and $\delta^{15}N$), *PLoS ONE*, *10*, e0131555.

Carricart-Ganivet, J., J. L. Vasquez-Bedoya, N. Cabanillas-Teran, and P. Blanchon (2013), Gender-related differnces in the apparent timing of skeletal density bands in the reef-building coral *Siderastrea siderea*, *Coral Reefs*, *32*, 769-777.

Carvalho, M. C., I. R. Santos, D. T. Maher, T. Cryonak, A. McMahon, K. G. Schulz, and B. D. Eyre (2015), Drivers of carbon isotopic fractionation in a coral reef lagoon: Predominance of demand over supply, *Geochem. Cosmochem. Acta*, *153*, 105-115.

Castillo, K. D., J. B. Ries, and J. M. Weiss (2011), Declining coral skeletal extension for forereef colonies of *Siderastrea siderea* on the Mesoamerican Barrier Reef system, Southern Belize, *Plos one*, *6*(2), e14615.

Castillo, K. D., J. B. Ries, J. F. Bruno, and W. I.T. (2014), The reef-building coral *Siderastrea siderea* exhibits parabolic responses to ocean acidification and warming, *Proceedings of the Royal Society of London B*, *281*, 20141856.

Costanza, R., R. de Groot, P. Sutton, S. van der Ploeg, S. J. Anderson, I. Kubiszewski, S. Farber, and R. K. Turner (2014), Changes in teh global value of ecosystem services, *Global. Environ. Change*, *26*, 152-158.

DeCarlo, T. M., A. L. Cohen, G. T. F. Wong, F.-K. Shiah, S. J. Lentz, K. A. Davis, K. E. Shamberger, and P. Lohmann (2017), Community production modulates coral reef pH and the sensitivity of ecosystem calcification to ocean acidification, *J. Geophys. Res. Oceans*, *122*, 745-761.

Dickson, A. G. (1990), Thermodynamics of the dissociation of boric acid in synthetic seawater from 273.15 to 318.15 K, *Deep Sea Research Part A. Oceanographic Research Papers*, *37*(5), 755-766.

D'Olivo, J. P., M. T. McCulloch, S. Eggins, and J. Trotter (2015), Coral records of reef-water pH across the central Great Barrier Reef, Australia: assessing the influence of river runoff on inshore reefs, *Biogeosciences*, *12*, 1223-1236.

Drupp, P. S., E. Heinen De Carlo, F. T. Mackenzie, C. L. Sabine, R. A. Feely, and K. E. Shamberger (2013), Comparison of CO_2 dynamics and air-sea gas exchange in differing tropical reef environments, *Aquatic geochemistry*.

Foster, G. L. (2008), Seawater pH, pCO_2 and $[CO_3^{2-}]$ variations in the Caribbean Sea over the last 130 kyr: A boron isotope and B/Ca study of planktic foraminifera, *Earth Planet. Sci. Lett., 271*, 254-266.

Foster, G. L., and J. W. B. Rae (2016), Reconstructing ocean pH with boron isotopes in foraminifera, *Annual Review of Earth and Planetary Science, 44*, doi: 10.1146/annurev-earth-060115-012226.

Foster, G. L., B. Honisch, G. Paris, G. S. Dwyer, J. W. B. Rae, T. Elliott, J. Gaillardet, N. G. Hemming, P. Louvat, and A. Vengosh (2013), Interlaboratory comparison of boron isotope analysis of boric acid, seawater and marine $CaCO_3$ by MC-ICPMS and NTIMS, *Chem. Geol., 358*, 1-14.

Gagan, M. K., A. R. Chivas, and P. J. Isdale (1994), High-resolution isotopic records from corals using ocean temperature and mass-spawning chronometers, *Earth Planet. Sci. Lett., 121*, 549-558.

Garnder, T. A., I. M. Cote, J. A. Gill, A. Grant, and A. R. Watkinson (2003), Long-term region-wide declines in Caribbean corals, *Science, 301*, 958-960.

Gattuso, J.-P., M. Frankignoulle, and S. V. Smith (1999), Measurement of community metabolism and significance in teh coral reef CO_2 source-sink debate, *Proceedings of the National Academy of Science, 96*, 13017-13022.

Gattuso, J.-P., et al. (2015), Contrasting futures for ocean and society from different anthropogenic CO_2 emission scenarios, *Science, 349*, aac4722-1 - aac4722-10.

Goodkin, N. F., B.-S. Wang, C.-F. You, K. A. Hughen, N. Grumet-Prouty, N. R. Bates, and S. C. Doney (2015), Ocean circulation and biogeochemistry moderate interannual and decadal surface water pH changes in the Sargasso Sea, *Geophycial Research Letters, 42*, 4931-4939.

Hemming, N. G., T. P. Guilderson, and R. G. Fairbanks (1998), Seasonal variations in the boron isotopic composition of coral: A productivity signal?, *Global Biogeochemical cycles, 12*(4), 581-586.

Holcomb, M., A. A. Venn, E. Tambutte, D. Allemand, J. Trotter, and M. T. McCulloch (2014), Coral calcifying fluid pH dictates response to ocean acidification, *Scientific Reports, 4*(5207), 1-4.

Hughes, T. P. (1994), Catastrophes, phase shifts, and large-scale degradation of a Caribbean coral reef, *Science, 265*, 1547-1551.

Jury, M. R. (2009), A quasi-decadal cycle in Caribbean climate, *J. Geophys. Res., 114*, D13102.

Keeling, C. D., W. G. Mook, and P. R. Tans (1979), Recent trends in the $^{13}C/^{12}C$ ratio of atmospheric carbon dioxide, *Nature, 277*, 121-123.

Klochko, K., A. J. Kaufman, W. Yoa, R. H. Byrne, and J. A. Tossell (2006), Experimental measurement of boron isotope fractionation in seawater, *Earth Planet. Sci. Lett., 248*, 261-270.

Krief, S., E. J. Hendy, M. Fine, R. Yam, A. Meibom, G. L. Foster, and A. Shemesh (2010), Physiological and isotopic responses of scleractinian corals to ocean acidification, *Geochmica et Cosmochimca Acta, 74*, 4988-5001.

Kubota, K., Y. Yokoyama, T. Ishikawa, A. Suzuki, and M. Ishii (2017), Rapid decline in pH of coral calcification fluid due to incorporation of anthropogenic CO_2, Scientific Reports, 7: 7694, doi: 10.1038/s41598-017-07680-0.

Lavigne, L., and J.-P. Gattuso (2010), Seacarb: seawater carbonate chemistry with R, *R package version 2.4.3*.

Liu, Y., et al. (2014), Acceleration of modern acidification in the South China Sea driven by anthropogenic CO_2, *Scientific Reports*, *4*(5148), 1-5.

Meibom, A., et al. (2006), Vital effects in coral skeletal composition display strict three-dimensional control, *Geophysical Research Letters*, 33, L11608, doi: 10.1029/2006GL025968

Martin, P., N. F. Goodkin, J. A. Stewart, G. L. Foster, E. L. Sikes, H. K. White, S. Hennige, and J. M. Roberts (2016), Deep-sea coral $d^{13}C$: A tool to reconstruct the difference between seawater pH and d11B-derived calcification site pH., *Geophysical Research Letters*, *43*, 299-308.

McClanahan, T. R., R. Aronson, W. Precht, and N. Muthiga (1999), Fleshy algae dominate remote coral reefs of Belize, *Coral Reefs*, *18*, 61-62.

McConnaughy, T. (1989), ^{13}C and ^{18}O isotopic disequilibrium in biological carbonates: I. Patterns, *Geochimica et Cosmochimica Acta*, *53*, 151-162.

McCulloch, M. T., J. Falter, J. Trotter, and P. Montagna (2012), Coral resilience to ocean acidification and global warming through pH up-regulation, *Nature Climate Change*, *2*, 623-627.

Muscatine, L., J. W. Porter, and I. R. Kaplan (1989), Resource partitioning by reef corals as determined from stable isotope composition, *Marine Biology*, *100*, 185-193.

Noireaux, J., V. Mavromatis, J. Gaillardet, J. Schott, V. Montouillout, P. Louvat, C. Rollion-Bard, and D. R. Neuville (2015), Crystallographic control on the boron isotope paleo-pH proxy, *Earth Planet. Sci. Lett.*, *430*, 398-407.

Okai, T., A. Suzuki, H. Kawahata, S. Terashima, and N. Imai (2002), Preparation of a New Geological Survey of Japan Geochemical Reference Material: Coral JCp-1, *Geostandard Newslett.*, *26*, 95-99.

Pelejero, C., E. Calvo, M. T. McCulloch, J. F. Marshall, M. K. Gagan, J. M. Lough, and B. N. Opdyke (2005), Preindustrial to modern interdecadal variability in coral reef pH, *Science*, *309*, 2204-2207.

Rayner, N. A., D. E. Parker, E. B. Horton, C. K. Folland, L. V. Alexander, D. P. Rowell, E. C. Kent, and A. Kaplan (2003), Global analyses of sea surface temperature, sea ice and night marine air temperature since the late nineteenth century, *J. Geophys. Res.*, *108*, 4407.

Reynaud, S., C. Ferrier-Pages, R. Sambrotto, A. Juillet-Leclerc, J. Jaubert, and J.-P. Gattuso (2004), Effect of feeding on the carbon and oxygen isotopic composition of tissues and skeleton of the zooxanthellate coral *Stylophora pistillata Marine Ecology Progress Series*, *238*, 81-89.

Ries, J. B. (2011), A physicochemical framework for interpreting the biological calcification response to CO2-induced ocean acidification. *Geochimica et Cosmochimica Acta 75*, 4053-4064 .

Rollion-Bard, C., M. Chaussidon, and C. France-Lanord (2003), pH control on oxygen isotopic composition of symbiotic corals, *Earth Planet. Sci. Lett.*, 215, 275-288.

Rubino, M., et al. (2013), A revised 1000 year atmospheric $\delta^{13}C$-CO_2 record from Law Dome and South Pole, Antarctica *Journal of Geophysical Research: Atmospheres*, *118*, 8482-8499.

Sabine, C. L., et al. (2004), The oceanic sink for anthropogenic CO_2, *Science*, *305*, 367-371.

Schutte, V. G. W., E. R. Selig, and J. F. Bruno (2010), Regional spatio-temporal trends in Caribbean coral reef benthic communities, *Marine Ecology Progress Series*, *402*, 115-122.

Shinjo, R., R. Asami, K.-F. Huang, C.-F. You, and Y. Iryu (2013), Ocean acidification trend in the tropical North Pacific since the mid-20th century reconstructed from a coral archive, Marine Geology, 342, 58-64

Silverman, J., D. I. Kline, L. Johnson, T. Rivlin, K. Schneider, J. Erez, B. Lazar, and K. Caldeira (2012), Carbon turnover rates in the One Tree Island Reef: A 40-year perspective, *J. Geophys. Res.*, *117*(G03023).

Silverman, J., K. Schneider, D. I. Kline, T. Rivlin, A. Rivlin, S. Hamylton, B. Lazar, J. Erez, and K. Caldeira (2014), Community calcification in Lizard Island, Great Barrier Reef: A 33 year perspective, *Geochmica et Cosmochimca Acta*, *144*, 72-81.

Spero, H., J. Bijma, D. W. Lea, and B. E. Bemis (1997), Effect of seawater carbonate concentration on planktonic formainiferal carbon and oxygen isotopes, *Nature*, *390*, 497-500.

Stephenson, T. S., et al. (201), Changes in extreme temperature and precipitation in the Caribbean region, 1961-2010, *Int. J. Climatol.*, *34*, 2957-2971.

Swart, P. K. (1983), Carbon and oxygen isotope fractionation in scleractinian corals: a review, *Earth-Science Reviews*, *19*, 51-80.

Swart, P. K., L. Greer, B. E. Rosenheim, C. S. Moses, A. J. Waite, A. Winter, R. E. Dodge, and K. Helmle (2010), The ^{13}C Suess effect in scleractinian corals mirror changes in the anthropogenic CO_2 inventory of the surface ocean *Geophycial Research Letters*, *37*, L05604.

Takahashi, T., S. Sutherland, D. W. Chipman, J. G. Goddard, C. Ho, T. Newberger, C. Sweeney, and D. R. Munro (2014), Climatological distributions of pH, pCO2 , total CO2, alkalinity, and CaCO3 saturation in the global surface ocean, and temporal changes at selected locations, Mar. Chem., 164, 95-125.

Titlyanov, E. A., S. I. Kiyashko, T. V. Titlyanova, and J. A. Raven (2010), $\Delta^{13}C$ and $\delta^{15}N$ in tissue of coral polyps and epilithic algae inhabiting damaged coral colonies under the influence of different light intensities, *Aquat. Ecol.*, *44*, 13-21.

Trotter, J., P. Montagna, M. T. McCulloch, S. Silenzi, S. Reynaud, G. Mortimer, S. Martin, C. Ferrier-Pages, J.-P. Gattuso, and R. Rodolfo-Metalpa (2011), Quantifying the pH "vital effect" in temperate zooxanthellate coral *Cladocora caespitosa*: Validation of the boron seawater pH proxy, *Earth Planet. Sci. Lett.*, *303*, 163-173.

Venn, A. A., E. Tambutte, M. Holcomb, J. Laurent, D. Allemand, and S. Tambutte (2013), Impact of seawater acidification on pH at the tissue-skeleton interface and calcification in reef corals, *Proceedings of the National Academy of Science*, *110*(5), 1634-1639.

Wei, G., M. T. McCulloch, G. Mortimer, W. Deng, and L. Xie (2009), Evidende for ocean acidification in the Great Barrier Reef of Australia, *Geochmica et Cosmochimca Acta*, *73*, 2332-2346.

Wei, G., Z. Wang, T. Ke, Y. Liu, W. Deng, X. Chen, J. Xu, T. Zeng, and L. Xie (2015), Decadal variability in seawater pH in the West Pacific: Evidence from coral $\delta^{11}B$ records, *J. Geophys. Res. Oceans*, *120*, 7166-7181.

Yeakel, K. L., A. J. Andersson, N. R. Bates, T. J. Noyes, A. Collins, and R. Garley (2015), Shifts in coral reef biogeochemistry and resulting acidification linked to offshore productivity, *Proceedings of the National Academy of Science*, *112*, 14512-14517.

Zeebe, R., and D. A. Wolf-Gladow (2001), *CO_2 in Seawater: Equilibrium, Kinectics, Isotopes*, 346 pp., Elsevier, Amesterdam.

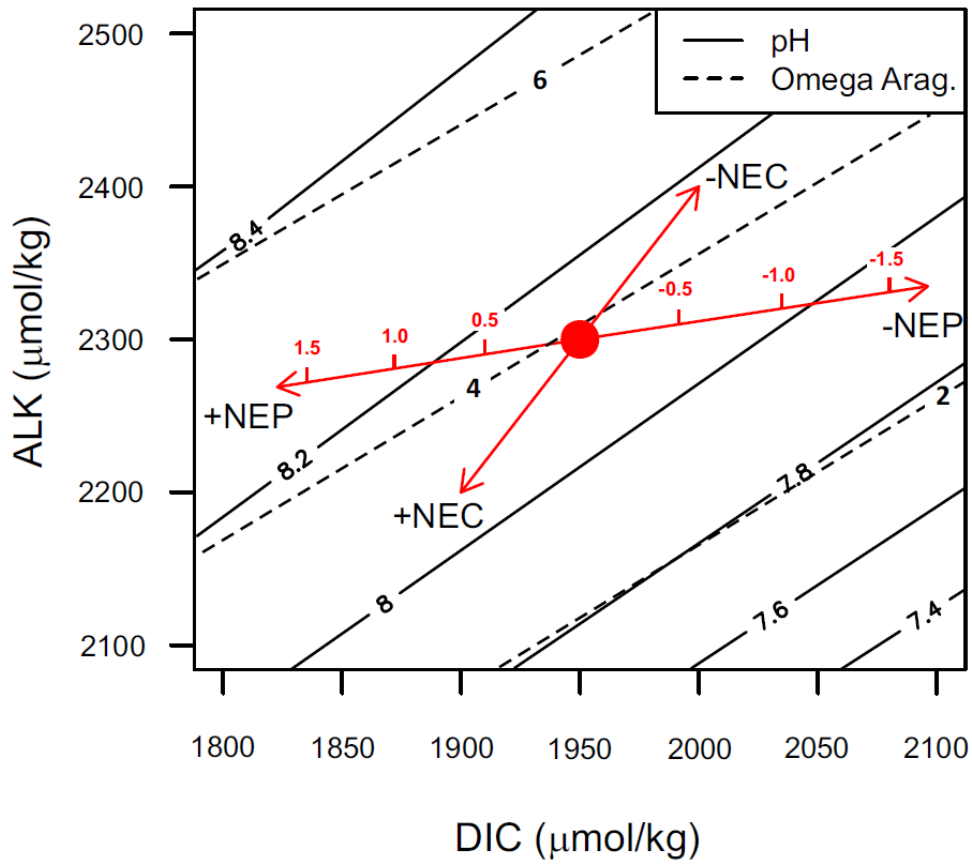

Figure 1. Plot of total alkalinity (ALK) vs. total dissolved inorganic carbon (DIC) contoured with pH (solid) and $\Omega_{aragonite}$ (dashed) and calculated at 25 ^{o}C, 35 psu and atmospheric pressure. The red lines show the influence of NEP and NEC on ALK and DIC. The central red dot represents an arbitrary starting point with the arrows showing the direction of change for increase/decrease (+/-) in NEC and NEP. One mole of $CaCO_3$ production on the reef removes 2 moles of ALK and 1 mole of DIC, whereas dissolution of $CaCO_3$ does the reverse. Reef primary production removes 1 mol of DIC as CO_2 and respiration does the opposite, with minimal effect on ALK [*Zeebe and Wolf-Gladrow*, 2001]. The NEP arrow has ticks that show the change in $\delta^{13}C$ of DIC caused by the removal/addition of organic carbon with a $\delta^{13}C$ of -24 ‰.

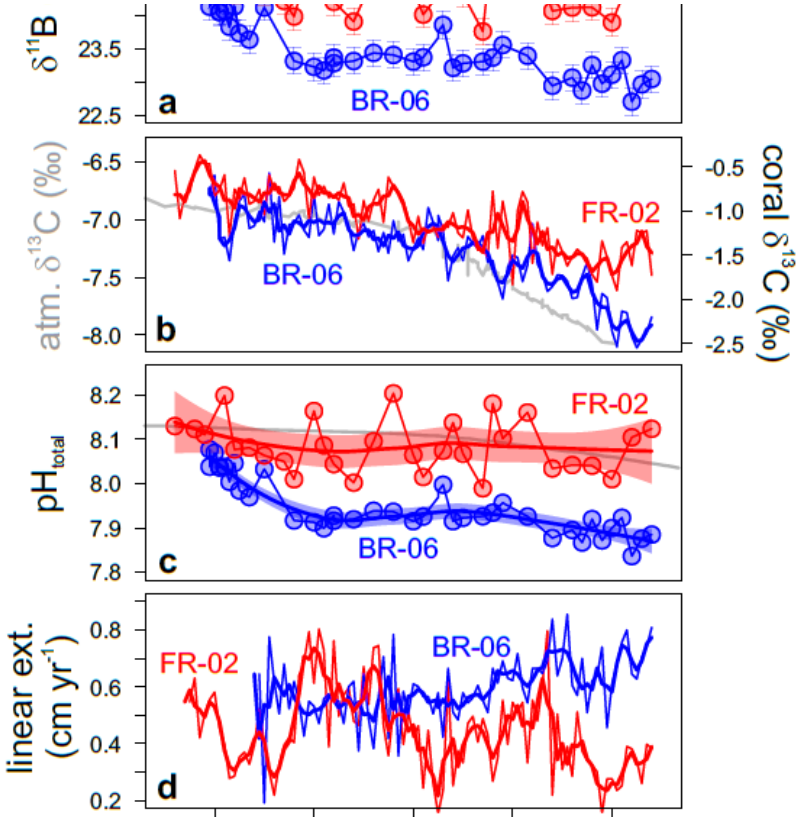

Figure 2. Geochemical data from forereef (FR-02; red) and backreef (BR-06, blue) cores of the scleractinian coral *S. siderea* from the southern MBRS, Belize, spanning 1910 to 2010. **a**. Boron isotope ($\delta^{11}B$) data with error bars representing analytical uncertainty. **b**. The carbon isotope ($\delta^{13}C$) composition of atmospheric CO_2 from *Rubino et al.* [2013] (grey line, left axis) and annually resolved $\delta^{13}C$ of forereef (FR-02; red) and backreef (BR-06; blue) coral cores (right axis). Thick lines for the coral data are 3-point running means. **c**. Seawater pH derived from the coral $\delta^{11}B$ data plotted in panel a (see text for details). Grey line is seawater pH calculated for the past century from atmospheric pCO_2, the HadISST seawater temperature record, an assumed total of alkalinity of 2300 µmol/kg, and an assumed salinity of 35 psu. Also shown are LOESS best fit lines and 95% confidence intervals, with degree of smoothing determined by generalized cross validation. **d**. Linear extension of forereef (FR-02; red) and backreef (BR-06; blue) corals as reported by *Castillo et al.* [2011], with thick lines showing the 3-point running mean.

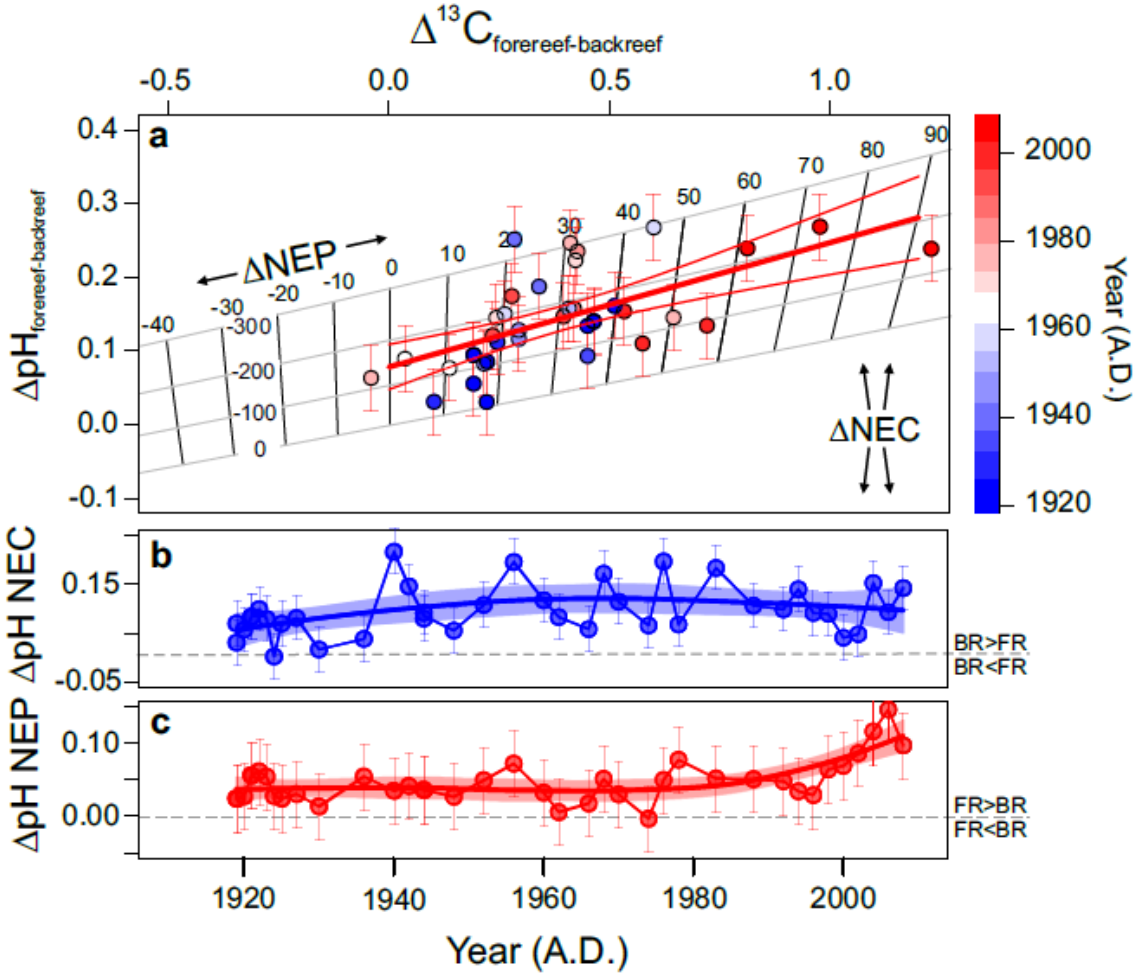

Figure 3. a. The relative evolution of δ^{11}B-derived seawater pH and δ^{13}C in the forereef and backreef of the southern MBRS, Belize. The timeseries from the backreef and forereef cores plotted in Figure 2 were interpolated onto a common age scale, permitting calculation of the forereef-to-backreef difference in seawater pH and δ^{13}C (ΔpH and Δ^{13}C, respectively). Each datum is colour-coded for year, as shown on scale to right. Error bars are quadratic sum of the uncertainty relating to the δ^{11}B measurement (± 0.02 pH units) and an assumed but conservative uncertainty in the pH-δ^{11}B calibration (±0.04 pH units). The plot is contoured by assuming a starting condition of DIC = 2000 µmol/kg and pH = 8.16, with the removal or addition of DIC via changing NEP shown by black lines and the removal or addition of ALK:DIC at a 2:1 ratio via changing NEC shown by grey lines. Contours are labeled with µmol/kg change in either DIC or ALK. It is assumed that NEC has no effect on δ^{13}C of seawater DIC and that organic carbon has δ^{13}C = -24 ‰ (*Briand et al.*, [2015]). Thick red line is best-fit least squares regression (with associated 95% confidence interval) through ΔpH and Δ^{13}C data. **b**. Estimated pH change caused by changing NEC only. ΔpH > 0 indicates of higher NEC in the backreef and vice versa. **c**. Estimated pH change caused by changing NEP only. ΔpH > 0 indicates higher NEP in the forereef and vice versa. Error bars in **b** and **c** are ca. ± 0.05 pH units at 95% confidence as in **a**.